Predicting Membrane Flux of CH_4 and CF_4 Mixtures in Faujasite from Molecular Simulations

Martin J. Sanborn and Randall Q. Snurr
Dept. of Chemical Engineering, Center for Catalysis and Surface Science, Northwestern University, Evanston, IL 60208

The Fickian transport diffusivities of binary mixtures of methane and CF_4 in the zeolite faujasite were investigated as a function of composition and loading. Using equilibrium molecular dynamics simulations, transport diffusivities of the mixtures were calculated from linear response theory. At low loadings, the diffusive cross terms are an order of magnitude smaller than the diffusive main terms, but at higher loadings they are on the same order of magnitude. The main term diffusivities are weak functions of concentration. The transport diffusivities were fitted as a function of adsorbate concentrations and used in the Fickian flux equations to predict codiffusion, counterdiffusion, and osmotic diffusion through a perfectly crystalline faujasite membrane. The osmotic and counterdiffusion cases show that it is critical to include both the cross term and main term diffusivities to predict the correct behavior. The permeances of methane and CF_4 through the faujasite membrane are reported.

Introduction

Zeolite membranes have been an area of intense research in recent years (Tavolaro and Drioli, 1999), largely because zeolites have several desirable properties that make them attractive membrane candidates, including their adsorption and shape selectivity characteristics. The idea of molecular traffic control (Clark et al., 2000) has intriguing possibilities as well that could possibly be exploited in membrane technology. Understanding diffusion through zeolite membranes is critical for their application in separations and catalysis. Used in conjunction with experiments, molecular simulations can be a powerful tool for gaining insight into the diffusion processes within zeolite membranes. Simulations can be used to predict diffusion coefficients which are then used in an appropriate theoretical framework for multicomponent diffusion. The simulation may also provide molecular-level details of sorbate motion within the zeolite.

Multicomponent diffusion can be described by a number of different frameworks. These include the generalized Maxwell-Stefan (GMS) formulation, the Fickian formulation, and Onsager's formulation derived from irreversible thermodynamics. All three are described by Taylor and Krishna (1993). Theodorou et al. (1996) discuss the calculation of Fickian diffusivities from linear response theory with regard to microporous materials in particular, and Krishna and Wesselingh (1997) have written a comprehensive review of the GMS approach to mass transfer, including its use to describe diffusion in zeolites.

The diffusion coefficients that go into these models are referred to here as "transport" diffusivities to indicate their nonequilibrium nature and to distinguish them from the equilibrium self-diffusivities that are more commonly calculated in molecular simulations (Kärger and Ruthven, 1992). Transport diffusivities can be calculated from either nonequilibrium or equilibrium simulation techniques, and both have been described in the literature. Maginn et al. (1993) used two different nonequilibrium techniques, gradient relaxation molecular dynamics (GRMD) and color field nonequilibrium molecular dynamics (NEMD), to calculate the transport diffusivity of methane in silicalite. In GRMD, a concentration gradient is established at the beginning of the simulation and allowed to relax. By following the relaxation of the gradient, the transport diffusivity can be obtained. In color field NEMD, the transport diffusivities are obtained by measuring the response of the system to a perturbing field and relating

Correspondence concerning this article should be addressed to R. Q. Snurr.

it to the corrected diffusivity. Another nonequilibrium method, known as dual control volume grand canonical molecular dynamics (DCV-GCMD), was introduced by Heffelfinger and van Swol (1994). In this technique, two control volumes are established in the simulation in which the chemical potentials are fixed by grand canonical Monte Carlo (GCMC) insertions and deletions. A chemical potential gradient can be established by fixing the chemical potentials of the two control volumes at two different values. Hence, a nonequilibrium concentration gradient is directly simulated. Equilibrium molecular dynamics (MD) simulations can also be used to calculate the transport diffusivity in zeolites. This was demonstrated recently for argon in $AlPO_4$-5 (Hoogenboom et al., 2000) and for mixtures of methane and CF_4 in faujasite (Sanborn and Snurr, 2000). The latter study included the explicit calculation of the binary cross term diffusivities. For systems where diffusion of clusters is the primary mode of transport, Sholl (2000) has shown that the diffusion coefficients may be calculated using a coarse-grained model by examining the autocorrelation function of cosine transform fluctuations.

Various simulations have been used to study the flux of single and multicomponent systems through zeolite membranes. Pohl et al. (1996) used the DCV-GCMD method to simulate the transport of He, H_2, or CH_4 across ZSM-5 membranes, and found their results to compare favorably with several experimental results including those of Krishna and van den Broeke (1995). Suzuki et al. (2000) studied gas permeance of pure methane or ethylene through a silicalite membrane by calculating self-diffusivities using Monte Carlo techniques and then using the self-diffusivity results and Maxwell-Stefan theory to calculate transport diffusivities. Sholl (2000) predicted the flux across an ideal zeolite crystal for pure Xe and pure CF_4 in $AlPO_4$ by first calculating the transport diffusivities of atom clusters in the zeolite, then using the transport diffusivities to solve the Fickian flux equation. Kapteijn et al. (1995) studied the permeation of pure C1 to C5 alkanes through a silicalite membrane and used generalized Maxwell-Stefan theory to model the diffusion of binary mixtures in terms of only the pure component diffusivities. Krishna and van den Broeke (1995) modeled transient permeation flux data of light hydrocarbons through silicalite-1 membranes in terms of Maxwell-Stefan diffusion theory, and Krishna et al. (1998) demonstrated that a mixture of hexane and 2-methylpentane could be separated based upon preferential adsorption of the linear hexane in silicalite membranes. They estimated the membrane selectivities based on GMS theory, using configurational-bias Monte Carlo (CBMC) to calculate the adsorption isotherms for both the single component and mixture systems. Separation of various binary mixtures using a silicalite-1 membrane was also modeled by van den Broeke et al. (1999) using Maxwell-Stefan theory.

Kapteijn et al. (1995), Krishna and van den Broeke (1995), and van den Broeke et al. (1999) ignored the cross term diffusivities when predicting the membrane flux, assuming that sorbates could not pass one another in the zeolite channels. While this may be acceptable for those particular systems and conditions, neglecting these cross terms in general may not be accurate. For example, Carlson and Dranoff (1986) measured the uptake of a methane and ethane mixture in 4A zeolite and fit both the main and cross term diffusivities to the data. While the cross term diffusivities were many orders of magnitude smaller than the main terms at 322 K, the cross term diffusivities differed only by a single order of magnitude at room temperature. Using molecular dynamics simulations, both the main and cross term contributions can be calculated explicitly for the multicomponent system with no assumptions other than those in the potential model of the simulation. With the explicit cross terms available, the appropriateness of ignoring the cross terms can be investigated.

The objective of this article is to demonstrate how molecular dynamics (MD) may be used to predict the flux through a zeolite membrane by calculating both the main and cross term transport coefficients. In particular, the transport diffusivities of binary mixtures of CF_4 and methane in faujasite are studied as a function of loading and composition. Faujasite is a large pore zeolite whose unit cell consists of 8 tetrahedrally connected supercages of 12 Å in diameter. The main and cross term transport diffusivities calculated from the equilibrium MD simulations are used to predict flux through a faujasite membrane. These flux calculations demonstrate the importance of the cross term diffusivities for a correct description of flux behavior.

Diffusion Theory

The Fickian description of flux for a binary mixture in a zeolite system is

$$\begin{aligned} \boldsymbol{J}_i &= -D_{ii}\nabla c_i - D_{ij}\nabla c_j \\ \boldsymbol{J}_j &= -D_{ji}\nabla c_i - D_{jj}\nabla c_j \end{aligned} \tag{1}$$

where $\boldsymbol{J}_i$ is the flux of component i, D_{ii} is the main-term diffusivity, D_{ij} is the cross-term diffusivity, and c_i is the concentration of species i. The cross term diffusivities D_{ij} and D_{ji} are not necessarily equal. From a simulation standpoint, it is more convenient to express Eq. 1 in terms of phenomenological coefficients and chemical potential gradients

$$\boldsymbol{J}_i = -L_{ii}\nabla\mu_i - L_{ij}\nabla\mu_j, \tag{2}$$

where L is the phenomenological coefficient and μ is the chemical potential. According to the Onsager (1931a,b) reciprocal relations

$$L_{ij} = L_{ji}. \tag{3}$$

This provides a convenient check for the correctness of the simulation results.

The phenomenological coefficients may be calculated using linear response theory (Theodorou et al., 1996). According to linear response theory

$$L_{ij} = \frac{1}{3Vk_BT}\int_0^\infty \langle \boldsymbol{j}_i(0)\cdot\boldsymbol{j}_j(t)\rangle dt, \tag{4}$$

where V is the volume, k_B is the Boltzmann constant, T is the system temperature, and $\boldsymbol{j}$ is the microscopic current defined as

$$\boldsymbol{j}_i = \sum_{l=1}^{N_i} \boldsymbol{v}_l, \tag{5}$$

with N_i equal to the number of molecules of species i and $\boldsymbol{v}_l$ the molecular velocity of molecule l. The microscopic currents are an equilibrium property of the system which can be obtained directly from equilibrium MD simulations. Equation 4 is of the Green-Kubo form, and the equivalent Einstein form can be found elsewhere (Theodorou et al., 1996).

If Eqs. 1 and 2 are combined, an expression for the transport diffusivities may be obtained. The chemical potentials in Eq. 2 can be replaced by the fugacities f using the expression

$$\mu - \mu_0 = k_B T \ln\left(\frac{f}{f_0}\right), \tag{6}$$

where μ_0 and f_0 are the chemical potential and fugacity at a given reference state. Combining this new result with Eq. 1 yields an expression for the transport diffusivities D in terms of L and f

$$\begin{aligned} D_{ii} &= \frac{k_B T}{c_i}\left[L_{ii}\left(\frac{\partial \ln f_i}{\partial \ln c_i}\right)_{T,c_j} + L_{ij}\left(\frac{\partial \ln f_j}{\partial \ln c_i}\right)_{T,c_j}\right] \\ D_{ij} &= \frac{k_B T}{c_j}\left[L_{ii}\left(\frac{\partial \ln f_i}{\partial \ln c_j}\right)_{T,c_i} + L_{ij}\left(\frac{\partial \ln f_j}{\partial \ln c_j}\right)_{T,c_i}\right]. \end{aligned} \tag{7}$$

The chemical potential, and, hence, the fugacity, can be calculated using the Widom (1963) insertion method. At random times throughout the MD simulation, a "ghost" particle is inserted into the system. This ghost particle does not interact with any other molecules in the system, and, as such, has no effect on the system. The total potential energy experienced by this ghost particle $\mathfrak{V}_{\text{test}}$ is calculated. For a system taken in the canonical (NVT) ensemble, the excess chemical potential may be calculated using

$$\mu^{\text{ex}} = -k_B T \ln\langle \exp(-\mathfrak{V}_{\text{test}}/k_B T)\rangle, \tag{8}$$

where angled brackets denote an ensemble average. The total chemical potential is simply the sum of the ideal and excess parts

$$\mu = \mu^{\text{id}} + \mu^{\text{ex}}. \tag{9}$$

The ideal part is given by the expression

$$\mu^{\text{id}} = -k_B T \ln\left(\frac{V}{\langle N\rangle \Lambda^3}\right) \tag{10}$$

where N is the number of molecules in the system and Λ is the thermal wavelength which is defined as

$$\Lambda = \frac{h}{(2\pi m k_B T)^{1/2}} \tag{11}$$

where h is Planck's constant, and m is the molecular mass.

Table 1. Lennard-Jones Potential Parameters Used in MD Simulations

Potential Term	σ (Å)	ϵ/k_B (K)	Ref.
CH_4-CH_4	3.73	147.95	Goodbody et al. (1991)
CF_4-CF_4	4.662	134.0	Reid et al. (1987)
CH_4-CF_4	4.196	140.9	Lorentz-Berthelot
CH_4-Zeolitic O	3.214	133.3	Goodbody et al. (1991)
CF_4-Zeolitic O	3.734	109.57	Snurr and Kärger (1997)

Model and Simulation Information

The model and simulation techniques used in this work are similar to those used previously (Sanborn and Snurr, 2000). A united atom model is used to describe methane and CF_4. Interactions are considered pairwise additive and described by a Lennard-Jones potential

$$\mathfrak{V}_{ij} = 4\epsilon_{ij}\left[\left(\frac{\sigma_{ij}}{r_{ij}}\right)^{12} - \left(\frac{\sigma_{ij}}{r_{ij}}\right)^{6}\right], \tag{12}$$

where $\mathfrak{V}_{ij}$ is the potential energy between centers i and j, and r_{ij} is the distance between the centers. Parameters σ and ϵ for the Lennard-Jones interactions are given in Table 1.

The Newtonian equations of motion were integrated using a sixth-order Gear predictor-corrector method. The time step used for the simulations was 5 fs, with excellent energy conservation. Simulations were performed in the NVT ensemble using the Nose-Hoover thermostat with $Q_{\text{Nosé}} = 4\ 184$ kJ/mol $\cdot$ps^2, and the simulation temperature was set at 300 K. The simulation cell consisted of 8 unit cells, and each unit cell was $24.258 \times 24.258 \times 24.258$ Å. The siliceous form of faujasite was used in the simulation, and the zeolite coordinates were taken from Hriljac et al. (1993). Sorbate-zeolite interactions were pretabulated and stored prior to the simulation in order to speed the simulation.

All MD runs were allowed to equilibrate for 2.5–3.75 ns before the production runs began. Production runs for calculating the phenomenological coefficients were 2.5 ns long, with position and velocity data stored every 10 steps for later analysis. A total of 25 MD simulations were performed for each system and the results averaged together for calculating the phenomenological coefficients for each of the systems. A typical system of 256 molecules and eight unit cells averaged a few hours on a 500 MHz Alpha processor workstation.

For each binary system, up to 4 additional MD simulations were performed. These were used to calculate the derivatives in Eq. 7 for the given composition and loading. To calculate the chemical potentials, Widom insertions were performed after the simulations using the stored configurations. The method used is similar to that of Snurr et al. (1991). Ghost molecules were inserted at regular points 1.17 Å apart in the simulation box. A total of 100 configurations for each simulation were used. Increasing the number of configurations used did not affect the calculated chemical potential. The chemical potentials calculated using the insertion method were identical to those calculated from grand canonical Monte Carlo (GCMC) simulations.

Results and Discussion

In order to simplify the discussion, methane will be referred to as component 1 and CF_4 will be referred to as component 2 throughout the discussion. For example, J_1 refers to the flux of methane, and c_2 refers to the concentration of CF_4.

Equation 7 shows that the transport diffusion coefficients consist of two types of factors, phenomenological and thermodynamic. The phenomenological, or L, coefficients for these systems have been presented elsewhere (Snurr et al., 2001). Both main term L coefficients were functions of composition. For methane, L_{11} increased an order of magnitude as the methane composition increased, while the CF_4 main term coefficient L_{22} decreased, but not as dramatically. At the highest loading of six molecules per supercage (s.c.), L_{22} was independent of composition. The cross term coefficients L_{12} and L_{21} were not a function of composition or loading. Moreover, L_{12} and L_{21} had the same value within the given simulation error, satisfying Eq. 3.

Next, consider the thermodynamic terms $d \ln f/d \ln c$. The thermodynamic terms are nearly independent of composition at low loadings of 2 and 4 molecules/s.c. At very high loading of 6 molecules/s.c., the thermodynamic terms $d \ln (f_2)/d \ln (c_2)$ and $d \ln (f_1)/d \ln (c_2)$ become strong functions of concentration, as seen in Figure 1. At such high loadings, the zeolite is nearly saturated with molecules. It is much easier to fit methanes into the zeolite than the more bulky CF_4 molecules. As the composition shifts from mostly methane to mostly CF_4, correspondingly high pressure changes, and, hence, fugacities, are needed to obtain a small increase in the loading. It should be noted that very high pressures are required to obtain loadings of 6 molecules/s.c., which may not be easily obtainable in the laboratory. However, the data are presented to demonstrate the loading dependence of the diffusion terms.

With the L coefficients and thermodynamic terms, Eq. 7 is used to calculate the transport diffusivities. The diffusivities as a function of composition are shown in Figures 2 through 5. The main term D_{11} increases with increasing methane composition and decreases slightly with increasing loading. The main term D_{22} appears to be only a weak function of composition. Neither main term is a strong function of loading. On the other hand, both cross terms, D_{12} and D_{21}, are strong functions of composition and total loading. At 1 and 2 molecules/s.c., the cross terms are an order of magnitude smaller than the main terms. It is important to note that, at the higher loadings of 4 and 6 molecules/s.c., the cross terms are on the same order of magnitude as the main terms. This suggests that they should not be neglected, particularly at high loadings.

Taylor and Krishna (1993) find that while in gaseous systems the cross terms are generally smaller than the main terms by an order of magnitude or more, this is not the case in bulk

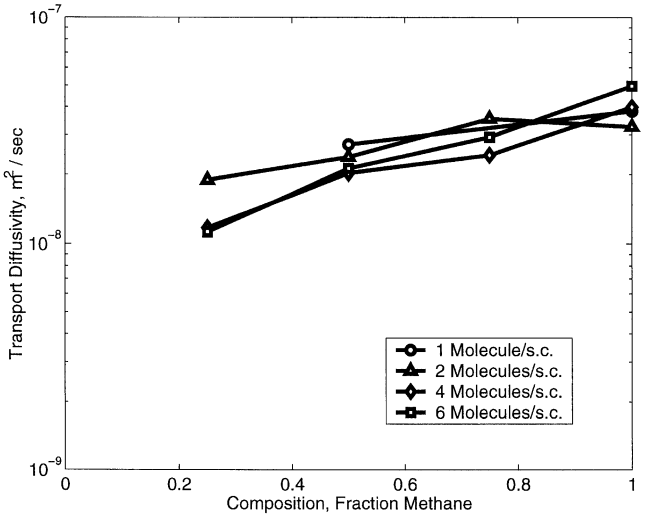

Figure 2. Main term diffusivities D_{11} as a function of composition at loadings of 1, 2, 4, and 6 molecules/s.c.

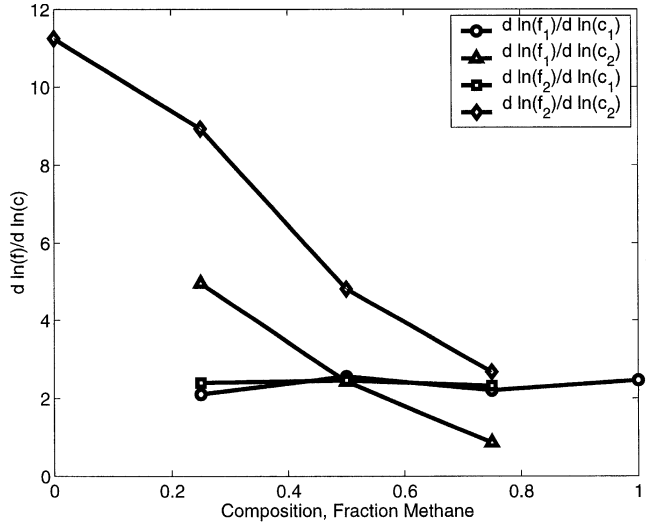

Figure 1. Thermodynamic terms at a loading of 6 molecules/s.c.

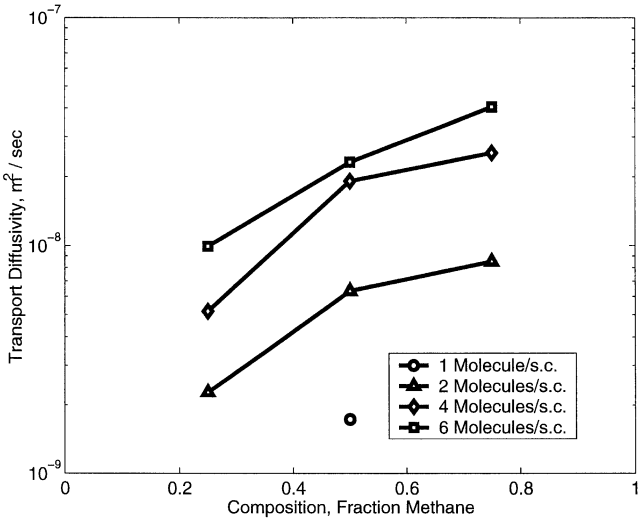

Figure 3. Transport diffusivity cross terms D_{12} plotted vs. methane composition.

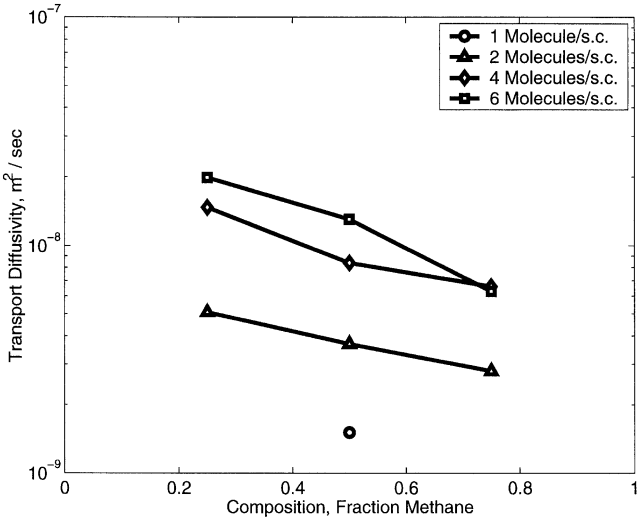

Figure 4. Transport diffusivity cross terms D_{21} plotted vs. methane composition.

liquids. Since the state of adsorbed molecules falls between these two extremes, one may expect that the cross terms play a role in the overall system behavior and may not be negligible in all cases. The cross term trends do indeed follow Krishna and Taylor's observation. In the zeolite at very high loadings, preferred adsorption sites along the walls are already filled, and additional sorbates must fill the centers of the supercages. These molecules behave more liquid-like than those adsorbed closer to the walls, and one can expect the cross terms to be on the same order of magnitude as the main terms like in bulk liquids.

It proved difficult to obtain consistent values for the L coefficients, and the related diffusivities, in two situations: first, for the minor component as the composition of the other component approached 100%, and, second, for all components when total mixture loadings were 1 molecule/s.c. In both cases, the correlation function of Eq. 4 was inconclusive. Attempts were made to improve the statistics of the correlations functions by increasing the total number of molecules simulated. The number of unit cells was increased to 64, but the Green-Kubo correlation function of Eq. 4 did not approach zero at long times, as is required. The simulation time step was reduced with no success, and the number of time steps between storing the positions and velocities was reduced by half also without success. In the cases where one component is in large excess of the other or the total system loading is low, a more efficient method for calculating the correlation functions is required. Nonequilibrium methods such as color field NEMD (Maginn et al., 1993) may be more appropriate. It is certainly of interest to study how the transport diffusivities behave as the mole fraction of the component of interest approaches zero.

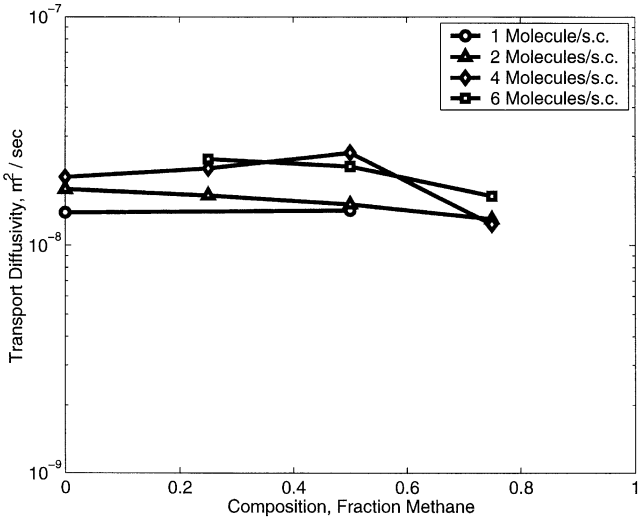

Figure 5. Transport diffusivity main terms D_{22} plotted vs. methane composition.

Application to Membrane Flux Calculations

To illustrate whether or not the cross terms are of importance in practical applications, this section investigates predicting the flux through a zeolite membrane utilizing the calculated transport diffusivities. As demonstrated in the previous section, MD simulations provide a means for calculating transport diffusivities, yielding a convenient method for predicting flux behavior in arbitrary adsorbate-zeolite systems.

The examples that follow will assume a perfectly crystalline faujasite membrane with no defects. Assume that the membrane is bounded in the x and y directions by an impenetrable boundary such that all measurable flux takes place in the z direction. This would correspond to a physical system in which the zeolite is embedded in an impermeable matrix, but open to the environment on the two z direction faces. Further assume the zeolite membrane to be in equilibrium with the gas phases such that the concentrations at the two boundaries are fixed. In this case, the fluxes in the z direction will be constant. Thus, given the boundary conditions, Eq. 1 can be solved for the fluxes and concentration gradients simultaneously.

While analytical solutions exist for the multicomponent Fickian flux equations, these are only valid for constant diffusivity D (Toor, 1964; Stewart and Prober, 1964). If D is a function of concentration, Eq. 1 must be solved numerically. To implement the numerical solution, the diffusivities reported in the previous section were fit to an empirical equation as a function of methane and CF_4 concentration using least squares

$$D_{ij} = a_0 + a_1 c_1^{e_1} + a_2 c_2^{e_2}. \tag{13}$$

The values of e were allowed to range from 0 to 4. The fit values are summarized in Table 2. It should be noted that these fits should not be used to predict diffusivities outside the range of the fitted data. The addition of more terms with different exponents to Eq. 13 did not significantly improve the fitting, nor did allowing the exponents to range greater than 4.

Since flux is assumed only in the z direction and the system is at steady state, Eq. 1 becomes an ordinary differential equation (ODE) of the boundary value problem (BVP) type. The shooting method for numerically solving BVPs was im-

Table 2. Fitted Parameters for Transport Diffusivities*

Transport Term	a_0	a_1	a_2	e_1	e_2
D_{11}	3.228	4.530×10^{7}	-1.001×10^{3}	3	1
D_{12}	−0.323	1.712×10^{3}	-1.027×10^{7}	1	3
D_{21}	−0.048	41.646	794.965	1	1
D_{22}	1.193	68.845	486.819	1	1

*The fits give diffusivity values in units of Å²/ps or $m^2/s\cdot10^{-8}$.

plemented (Press et al., 1992). In this method, the BVP is iteratively solved as an initial value problem (IVP), with initial guesses adjusted until the boundary conditions match. In this particular problem, the fluxes, $\boldsymbol{J}_1$ and $\boldsymbol{J}_2$, are guessed and the calculated end-point concentrations are compared to the specified boundary values. If the concentrations are not equal within a given tolerance, the fluxes are adjusted. A script for performing the shooting method was implemented in Matlab using in part the Matlab ode45 solver, an implementation of the fourth-order Runge-Kutta method.

Four flux cases are presented below. For each, the length of the membrane in the z-direction is 1 μm. First, co-diffusion of the two species is examined. Second is the case of osmotic diffusion. In osmotic diffusion, one component has a zero concentration gradient and the second has a nonzero concentration gradient. Contributions from the cross term diffusivities allow the component with no concentration gradient to have a nonzero flux. The third and fourth cases examine counterdiffusion. The boundary zeolite membrane concentrations, the corresponding gas-phase partial pressures, and the chemical potentials of the adsorbed phase are reported in Table 3. Recall that the chemical potential gradients are the true driving force for transport diffusion. Note that all the concentrations fall within the range of the fitted diffusivities.

In order to examine the importance of the various diffusion terms, four different diffusion models are used for each case: (I) both the main and cross term diffusivities are used; (II) only the main term diffusivities are used; (III) the pure component diffusivities are used in place of the multicomponent main term diffusivities, and the cross term diffusivities are ignored; and (IV), which is similar to model (II), but the main term phenomenological coefficients and chemical potential gradients are used in place of the diffusion coefficient and concentration gradients. Model (I) uses both the main and cross terms with the fitted parameters reported in Table 2. For model (II), the fitted parameters a_0, a_1, and a_2 for D_{12} and D_{21} were set to zero, ignoring any contribution from the cross term diffusivities. For model (III), only the pure component values in Figures 2 and 5 were fit to Eq. 13. The corresponding fitted parameters are presented in Table 4. The basis of model (IV) is Eq. 2. However, only the main term phenomenological coefficients L_{11} and L_{22} are considered. These coefficients were fitted as a function of chemical potential, again with the form of Eq. 13. These fitted parameters are reported in Table 5.

Table 3. Boundary Condition Concentrations (c_1, c_2), Gas-Phase Partial Pressures (p_1, p_2), and Chemical Potentials (μ_1, μ_2) of each Component at the Membrane Endpoints for the Various Cases Studied

z Position	c_1	c_2	p_1	p_2	μ_1	μ_2
μm	Molec./s.c.		kPa		kJ/mol	
			Codiffusion			
0	3.0	3.0	4 558.9	6627.0	−27.30	−32.75
1	0.5	0.5	210.0	93.0	−34.98	−43.39
			Osmotic diffusion			
0	2.5	1.0	1 309.6	302.2	−30.42	−40.45
1	1.0	1.0	454.2	227.7	−33.06	−41.16
			Counterdiffusion Case A			
0	2.5	1.0	1 309.6	302.2	−30.42	−40.45
1	1.0	2.5	633.6	1 214.5	−32.23	−36.98
			Counterdiffusion Case B			
0	2.5	1.0	1 309.6	302.2	−30.42	−40.45
1	2.0	2.5	1 568.7	1 777.2	−29.97	−36.03

Table 4. Fitted Parameters for Transport Diffusivities Using Only Single Component Data*

Transport Term	a_0	a_1	a_2	e_1	e_2
D_{11}	3.5261	3.758×10^{7}	0.0	3	–
D_{22}	1.278	0.0	334.345	–	1

*The fits give diffusivity values in units of Å²/ps or $m^2/s\cdot10^{-8}$.

A fifth diffusion model was also examined. For (V), Eq. 2 was used to describe the flux. The main term, L_{11} and L_{22}, and cross term, L_{12} and L_{21}, phenomenological coefficients were fit as functions of both methane and CF_4 chemical potential in a form analogous to Eq. 13. The flux calculation results were qualitatively identical to model (I), and the quantitative values were also very close to model (I). One would expect that the results be identical to model (I). However, limitations in fitting L_{11} to Eq. 13 prevented the results from exactly matching. An improved functional form for L_{11} could improve quantitative agreement of this model with (I).

Table 6 shows the calculated flux values for the co-diffusion case. All four models give qualitatively similar results. All predict positive values for $\boldsymbol{J}_1$ and $\boldsymbol{J}_2$, that is, flux from $z = 0$ toward $z = 1$ μm. Quantitatively, (II) underpredicts both fluxes, (III) underpredicts $\boldsymbol{J}_2$ and overpredicts $\boldsymbol{J}_1$, and (IV) underpredicts $\boldsymbol{J}_2$. The cross term diffusion coefficients enhance the flux of both components, and, in neglecting these terms, (II) underpredicts both fluxes. It is instructive also to examine the predicted composition profiles for models (I), (II), and (III), shown in Figure 6. When using (I), the CF_4 concentration profile has a pronounced curved shape, while the methane profile is only slightly curved. For (II), shown by the dashed line, both the methane and CF_4 profiles are slightly curved. The dotted line for (III) shows that the

Table 5. Fitted Parameters for Main Term Phenomenological Coefficients*

Phenomenological Term	a_0	a_1	a_2	e_1	e_2
L_{11}	0.0034	5.586×10^{-5}	2.769×10^{-5}	1	1
L_{22}	4.835×10^{-4}	3.762×10^{-6}	-5.482×10^{-11}	1	4

*The fits give L values in units of (molecules mol)/(ps kJ Å).

Table 6. Flux Values for Codiffusion of Methane and CF_4 through Faujasite Membrane

Model	J_1	J_2
	mol/cm^2·s	
(I)	0.27	0.22
(II)	0.19	0.15
(III)	0.30	0.14
(IV)	0.28	0.16

Table 7. Flux Values for Osmotic Diffusion of Methane and CF_4 through Faujasite Membrane

Model	J_1	J_2
	mol/cm^2·s	
(I)	0.14	0.02
(II)	0.14	0.0
(III)	0.18	0.0
(IV)	0.08	0.01

methane and CF_4 have nearly linear concentration profiles. If accurate concentration profiles were an important result to be obtained from the flux calculation, both the main and cross term diffusivities should be included.

The flux values for the osmotic diffusion case are reported in Table 7. This case highlights the importance of the diffusive cross term contribution. In only considering the main terms, both (II) and (III) predict there will be no flux of CF_4 across the membrane since $\nabla c_2 = 0$. However, when taking into account the cross term $-D_{21}\nabla c_1$, model (I) reveals that there is a small, but certainly not negligible, contribution to the flux $\boldsymbol{J}_2$. In this case, the cross term D_{21} creates the diffusion of component 2 across the membrane. If the chemical potential gradients, and not the concentration gradients, are examined for this case, it is clear that there will be diffusive flux of component 2 since $\nabla\mu_2$ is nonzero. Hence, (IV) correctly predicts that there is a flux associated with component 2.

The flux values for counterdiffusion case A are provided in Table 8. In this case, one component is in high concentration on each side of the membrane. All four diffusivity models give the same qualitative fluxes; that is, $\boldsymbol{J}_1$ is positive and $\boldsymbol{J}_2$ is negative. Quantitatively, (IV) nearly matches the values of (I), while (II) and (III) give $\boldsymbol{J}_1$ and $\boldsymbol{J}_2$ values that are 100–150% and 80% larger than (I), respectively. The errors in (II) and (III) are due to the absence of the cross terms which have a retarding effect on the flux of each component. Without their contribution, the predicted fluxes for (II) and (III) are larger than they should be.

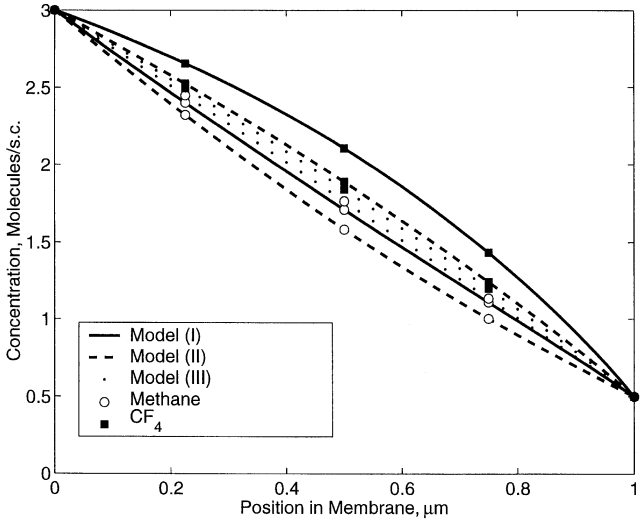

Figure 6. Codiffusion of methane and CF_4 in a faujasite membrane.

The open circles are the methane data and the closed squares are the CF_4 data.

The fluxes for counterdiffusion case B are reported in Table 9. The methane has a negative concentration gradient that is smaller than the positive CF_4 concentration gradient. The concentration profiles are shown in Figure 7. Although the fluxes are small, the cross terms play a very important role in this case. The cross term of the flux equation for $\boldsymbol{J}_1$, $-D_{12}\nabla c_2$, is larger than the main term, $-D_{11}\nabla c_1$, and the net flux is in the negative direction. Without taking the cross term into account, the fluxes predicted by (II) and (III) are not only quantitatively wrong, but qualitatively wrong, even predicting the wrong sign. The concentration gradients are misleading. As in the osmotic diffusion case, examining the chemical potentials in Table 3 reveals what behavior should be expected. Since the chemical potential gradients are both positive, one expects negative flux values for both components 1 and 2. Model (IV) does predict negative values for $\boldsymbol{J}_1$ and $\boldsymbol{J}_2$, although they differ quantitatively from (I).

The behavior seen in the osmotic diffusion case and the counterdiffusion case B is similar to some experimental results reported in the literature. For example, van de Graaf et al. (1999) found that if the cross term diffusivities of the GMS diffusion model were ignored when trying to predict the flux and membrane selectivity for ethane/methane and propane/methane mixtures in silicalite-1 membranes, the experimental data could not be quantitatively, or sometimes even qualitatively, described. Karimi and Farooq (2000) compared the use of GMS with and without the cross terms to describe binary diffusion through a membrane and found that the two models gave qualitative agreement, but quantitative agreement was limited to special circumstances.

It is of interest to inquire about the concentration dependence of the diffusivities, since the macroscopic calculations are much easier with constant diffusivities. How would the flux predictions change if a constant diffusivity were assumed? It is possible to make some preliminary conclusions even without calculating average diffusivity values. In Figures

Table 8. Flux Values for Counterdiffusion of CF_4 and Methane through Faujasite Membrane, Case A

Model	J_1	J_2
	mol/cm^2·s	
(I)	0.05	−0.05
(II)	0.11	−0.09
(III)	0.18	−0.08
(IV)	0.06	−0.05

Table 9. Flux Values for Counterdiffusion of Methane and CF_4 through Faujasite Membrane, Case B

Model	J_1	J_2
	mol/cm^2·s	
(I)	−0.051	−0.076
(II)	0.039	−0.089
(III)	0.061	−0.086
(IV)	−0.018	−0.067

2 and 5, the effect of concentration on the diffusivities is weak. As stated before, neither term is a strong function of loading or composition, so it would not be a poor assumption to use a constant diffusivity value for either D_{11} or D_{22} in the membrane flux calculations. The case is not as clear for the cross terms, since both D_{12} and D_{21} change an order of magnitude over the simulated range of compositions and loadings. Assuming a constant diffusivity for either of these terms will lead to quantitative errors when predicting membrane flux. Qualitative errors may occur as well, depending upon the values of D_{21} and D_{12}. This is especially true for counterdiffusion case B, where the flux of methane is highly dependent on the cross term diffusivity D_{12}.

There are only a small number of articles in the literature with experimental data for faujasite membranes, and none that correspond directly to the system studied here. It is instructive, however, to compare the permeance, which is commonly reported in the zeolite membrane literature, of other faujasite membrane experiments with the data compiled here. Table 10 shows the permeances corresponding to the fluxes calculated using model (I) for the different diffusion cases. The permeability of component i, $P_i^{\dagger}$, is defined as

$$P_i^{\dagger} = \frac{\delta N_i^{\text{tot}}}{A \Delta p_i}, \tag{14}$$

where δ is the membrane length, N_i^{tot} is the total moles of component i transferred per unit time, A is the area of the membrane, and Δp_i is the difference in partial pressure of component i across the membrane. If the membrane length is incorporated into the permeability, the new quantity is called the permeance. The permeance was calculated using

$$P_i = \frac{J_i}{\Delta p_i}, \tag{15}$$

where J_i is the scalar value of the flux of component i. Note that permeance is implicitly dependent upon membrane length.

Kusakabe et al. (1998) studied the separation of CO_2 from N_2 using NaY zeolite membranes at 313 K. They report average permeances on the order of 10^{-6}mol/(m^2·s·Pa) for CO_2, and 10^{-7}mol/(m^2·s·Pa) for N_2. In more recent work, Kusakabe et al. (1999) report permeances for CO_2 and N_2 mixtures in NaY zeolite membranes across a range of temperatures, as well as the permeances for methane, CO_2, C_2H_6, and C_3H_8 in equimolar binary mixtures with H_2 at 308 K. The methane mixture data are of most relevance here. For

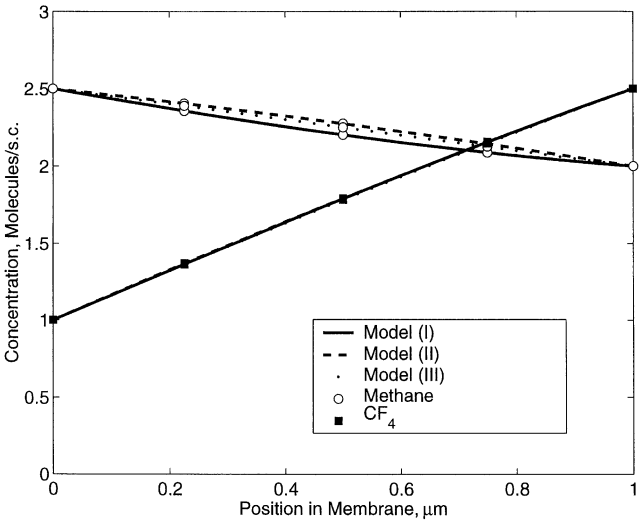

Figure 7. Counterdiffusion, case B, of methane and CF_4 through a zeolite membrane.

The open symbols are the methane data, and the closed symbols are the CF_4 data. While the flux of CF_4 is expected to be negative (oriented toward the $z = 0$ point), it is interesting to find that, due to the cross-term, the flux of methane is also negative.

methane in a binary mixture with H_2 in NaY zeolite, Kusakabe et al. report permeances of 2×10^{-7} mol/(m^2·s·Pa) for methane and 1×10^{-7} mol/(m^2·s·Pa) for H_2. The value for methane is significantly smaller than that reported in Table 10 for the codiffusion case, which resembles the separation experiments Kusakabe et al. performed. Kusakabe et al. had a partial pressure drop of around 50 kPa, while the pressure drops for the codiffusion case here were 4 000–6 000 kPa, significantly higher. In order to make a more direct comparison, an additional case of codiffusion through the idealized zeolite membrane was studied using model (I). The pressure drop for each component was fixed at 50 kPa, as in Kusakabe et al. However, the corresponding experimental concentrations for the methane and H_2 components were outside the range of the fitted methane and CF_4 diffusivities, so the same gas phase partial pressures could not be studied. The endpoint concentrations and gas-phase partial pressures used in the calculations are given in Table 11. The resulting fluxes and permeances are given in Table 12. Again, the methane permeance is much larger than that reported by Kusakabe et al.

It is important to realize that Kusakabe et al. (1999) only report permeance, not permeabilities, since the thickness of their membrane was unknown. It is the experimental perme-

Table 10. Permeance for Methane and CF_4 through Idealized Faujasite Membrane with Thickness of 1 μm

Diffusion Case	P_1	P_2
	mol/(m^2·s·Pa)	
Codiffusion	6.30×10^{-4}	3.38×10^{-4}
Osmotic diffusion	16.0×10^{-4}	29.5×10^{-4}
Counterdiffusion A	7.40×10^{-4}	5.48×10^{-4}
Counterdiffusion B	19.8×10^{-4}	5.17×10^{-4}

Table 11. Boundary Condition Concentrations (c_1, c_2) and Gas-Phase Partial Pressures (p_1, p_2) of Each Component at the Membrane Endpoints for Comparison with the Kusakabe Experiments

Membrane Position	c_1	c_2	p_1	p_2
	Molec/s.c.		kPa	
$z = 0$	0.61	0.73	260.0	143.0
$z = 1$ μm	0.5	0.5	210.0	93.0

ability that should be compared with the predicted permeability since permeability is independent of membrane length. Differences in the permeances may also be attributed to the fact that a siliceous form of faujasite was simulated in this article vs. the NaY zeolite studied by Kusakabe et al. Entrance effects may play an important role as molecules diffuse into and out of the zeolite and should be considered as well (Ford and Glandt, 1995a,b). Discrepancies in experimental and simulated permeances have also been reported by Pohl et al. (1996). The permeances they found using DCV-GCMD simulations of methane through ZSM-5 membranes were about 40 times larger than those obtained experimentally. Further study will be required to account for all the difference in permeances. It should be noted that the model used in this article predicts methane self-diffusivity in NaX well compared to PFG NMR results (Clark et al., 1999). PFG NMR experiments for mixtures are in progress in our lab to further validate the model.

Conclusions

It has been demonstrated that molecular simulations provide a convenient way to predict the binary fluxes of small molecules through zeolite membranes. Equilibrium molecular dynamics simulations were used to calculate the transport diffusivities of methane and CF_4 mixtures in faujasite utilizing linear response theory. It was shown that the cross term diffusivities play a more important role at high loadings, as they reach the same order of magnitude as the main terms. It was, however, found to be difficult to obtain transport diffusivities when one component has close to zero composition or at low total loadings using this equilibrium MD method.

Using only the transport diffusivities from molecular simulations as inputs for the macroscopic Fickian diffusion equations, predictions for the fluxes of methane and CF_4 mixtures through a faujasite membrane were reported. Neglecting the cross terms in the Fickian flux equations leads to quantitative errors. In some cases, neglecting the cross terms causes qualitative errors as well, such as predicting the wrong sign for the flux. It is important to take into account all diffusive terms, both main and cross, when calculating fluxes in multicomponent zeolite systems. If, instead, the phenomenological coefficients and chemical potential gradients are used to describe the flux, considering only the main term contributions may be acceptable in some cases. For the flux cases examined, using only the main term phenomenological coefficients to predict the flux yielded the correct qualitative behavior, but differed quantitively from the values obtained using both the main and cross term diffusivities.

When compared to the closest experimental data available, the permeance of methane in binary mixtures with CF_4 reported here was much higher than the permeance of methane in binary mixtures with H_2 reported by Kusakabe et al. (1999). Several differences in the simulations and experiments may account for some of the discrepancies.

Table 12. Fluxes and Permeances for Codiffusion of Methane and CF_4 through 1 μm Thick Faujasite Membrane for Comparison with the Kusakabe Experiments

	J	P
	mol/cm^2·s	mol/(m^2·s·Pa)
Methane	1.47×10^{-4}	2.94×10^{-5}
CF_4	1.45×10^{-4}	2.91×10^{-5}

Acknowledgments

The authors are grateful to the donors of the Petroleum Research Fund, administered by the American Chemical Society, for partial support of this work.

Literature Cited

Carlson, N. W., and J. S. Dranoff, "Competitive Adsorption of Methane and Ethane on 4A Zeolite," *Proc. Eng. Foundation Conf. on Fundamentals of Adsorption*, AIChE, New York (1986).

Clark, L. A., G. T. Ye, A. Gupta, L. L. Hall, and R. Q. Snurr, "Diffusion Mechanisms of Normal Alkanes in Faujasite Zeolites," *J. Chem. Phys.*, **111**, 1209 (1999).

Clark, L. A., G. T. Ye, and R. Q. Snurr, "Molecular Traffic Control in a Nanoscale System," *Phys. Rev. Lett.*, **84**, 2893 (2000).

Ford, D. M., and E. D. Glandt, "Molecular Simulation Study of the Surface-Barrier Effect—Dilute Gas Limit," *J. Phys. Chem.*, **99**, 11543 (1995a).

Ford, D. M., and E. D. Glandt, "Steric Hindrance at the Entrances to Small Pores," *J. Memb. Sci.*, **107**, 47 (1995b).

Goodbody, S. J., K. Watanabe, D. MacGowan, J. P. R. B. Walton, and N. Quirke, "Molecular Simulation of Methane and Butane in Silicalite," *J. Chem. Soc. Faraday Trans.*, **87**, 1951 (1991).

Heffelfinger, G. S., and F. van Swol, "Diffusion in Lennard-Jones Fluids Using Dual Control Volume Grand Canonical Molecular Dynamics Simulation (DCV-GCMD)," *J. Chem. Phys.*, **100**, 7548 (1994).

Hoogenboom, J. P., H. L. Tepper, N. F. A. van der Vegt, and W. J. Briels, "Transport Diffusion of Argon in AlPO4-5 from Equilibrium Molecular Dynamics Simulations," *J. Chem. Phys.*, **113**, 6875 (2000).

Hriljac, J. A., M. M. Eddy, A. K. Cheetham, J. A. Donohue, and G. J. Ray, "Powder Neutron Diffraction and ^{29}Si MAS NMR Studies of Siliceous Zeolite-Y," *J. Solid State Chem.*, **106**, 66 (1993).

Kapteijn, F., W. J. W. Bakker, G. Zheng, J. Poppe, and J. A. Moulijn, "Permeation and Separation of Light Hydrocarbons Through a Silicalite−1 Membrane: Application of the Generalized Maxwell-Stefan Equations," *Chem. Eng. J.*, **57**, 145 (1995).

Kärger, J., and D. M. Ruthven, *Diffusion in Zeolites and Other Microporous Solids*, Wiley, New York (1992).

Karimi, I. A., and S. Farooq, "Effect of Sorbate-Sorbate Interaction on Micropore Diffusion in Steady-State Adsorption Processes," *Chem. Eng. Sci.*, **55**, 3529 (2000).

Krishna, R., B. Smit, and T. J. H. Vlugt, "Sorption-Induced Diffusion-Selective Separation of Hydrocarbon Isomers Using Silicalite," *J. Phys. Chem. A*, **102**, 7727 (1998).

Krishna, R., and L. J. P. van den Broeke, "The Maxwell-Stefan Description of Mass Transport Across Zeolite Membranes," *Chem. Eng. J.*, **57**, 155 (1995).

Krishna, R., and J. A. Wesselingh, "The Maxwell-Stefan Approach to Mass Transfer," *Chem. Eng. Sci.*, **52**, 861 (1997).

Kusakabe, K., T. Kuroda, and S. Morooka, "Separation of Carbon Dioxide from Nitrogen Using Ion-Exchanged Faujasite-Type Zeolite Membranes Formed on Porous Support Tubes," *J. Memb. Sci.*, **148**, 13 (1998).

Kusakabe, K., T. Kuroda, K. Uchino, Y. Hasegawa, and S. Morooka, "Gas Permeation Properties of Ion-Exchanged Faujasite-Type Zeolite Membranes," *AIChE J*., **45**, 1220 (1999).
Maginn, E. J., A. T. Bell, and D. N. Theodorou, "Transport Diffusivity of Methane in Silicalite from Equilibrium and Nonequilibrium Simulations," *J. Phys. Chem*., **97**, 4173 (1993).
Onsager, L., "Reciprocal Relations in Irreversible Processes: I." *Phys. Rev*., **37**, 405 (1931a).
Onsager, L., "Reciprocal Relations in Irreversible Processes: II." *Phys. Rev*., **38**, 2265 (1931b).
Pohl, P. I., G. S. Heffelfinger and D. M. Smith, "Molecular Dynamics Computer Simulation of Gas Permeation in Thin Silicalite Membranes," *Molec. Phys*., **89**, 1725 (1996).
Press, W. H., S. A. Teukolsky, W. T. Vetterling, and B. P. Flannery, *Numerical Recipes in Fortran*: *The Art of Scientific Computing*, Cambridge University Press, New York (1992).
Reid, R. C., J. M. Prausnitz, and B. E. Poling, *The Properties of Gases and Liquids*, McGraw-Hill, New York (1987).
Sanborn, M. J., and R. Q. Snurr, "Diffusion of Binary Mixtures of CF_4 and *n*-Alkanes in Faujasite," *Sep. Pur. Tech*., **20**, 1 (2000).
Sholl, D., "Predicting Single-Component Permeance Through Macroscopic Zeolite Membranes from Atomistic Simulations," *Ind. Eng. Chem. Res*., **39**, 3737 (2000).
Snurr, R. Q., A. Gupta, and M. J. Sanborn, "Molecular Modeling of Multicomponent Diffusion in Zeolites," *First International Conference on Foundations of Molecular Modeling and Simulation*, P. T. Cummings, P. R. Westermoreland, B. Carnahan, eds., *AIChE Symp. Series*, **325**, 309 (2001).
Snurr, R. Q., R. L. June, A. T. Bell, and D. N. Theodorou, "Molecular Simulations of Methane Adsorption in Silicalite," *Molec. Sim*., **8**, 73 (1991).
Snurr, R. Q., and J. Kärger, "Molecular Simulations and NMR Measurements of Binary Diffusion in Zeolites," *J. Phys. Chem. B*, **101**, 6469 (1997).
Stewart, W. E., and R. Prober, "Matrix Calculation of Multicomponent Mass Transfer in Isothermal Systems," *Ind. Eng. Chem. Fund*., **3**, 224 (1964).
Suzuki, S., H. Takaba, T. Yamaguchi, and S. Nakao, "Estimation of Gas Permeability of a Zeolite Membrane, Based on a Molecular Simulation Technique and Permeation Model," *J. Phys. Chem. B*, **104**, 1971 (2000).
Tavolaro, A., and E. Drioli, "Zeolite Membranes," *Adv. Mater*., **11**, 975 (1999).
Taylor, R., and R. Krishna, *Multicomponent Mass Transfer*, Wiley, New York (1993).
Theodorou, D. N., R. Q. Snurr, and A. T. Bell, "Molecular Dynamics and Diffusion in Microporous Materials," *Comprehensive Supramolecular Chemistry*, Vol. 7, G. Alberti and T. Bein, eds., Pergamon, Oxford, pp. 507-548 (1996).
Toor, H. L., "Solution of the Linearized Equations of Multicomponent Mass Transfer: I," *AIChE J*., **10**, 448 (1964).
van de Graaf, J. M., F. Kapteijn, and J. A. Moulijn, "Modeling Permeation of Binary Mixtures through Zeolite Membranes," *AIChE J*., **45**, 497 (1999).
van den Broeke, L. J. P., F. Kapteijn, and J. A. Moulijn, "Transport and Separation Properties of a Silicalite-1 Membrane: II. Variable Separation Factor," *Chem. Eng. Sci*., **54**, 259 (1999).
Widom, B., "Some Topics in the Theory of Fluids," *J. Chem. Phys*., **39**, 2808 (1963).

Manuscript received Sept. 25, 2000 and revision received Mar. 23, 2001.